Scanning for velocity anomalies in the crust and mantle with diffractions from the core-mantle boundary — auxiliary material

Elmer Ruigrok, T. Dylan Mikesell and Kasper van Wijk

April 10, 2012

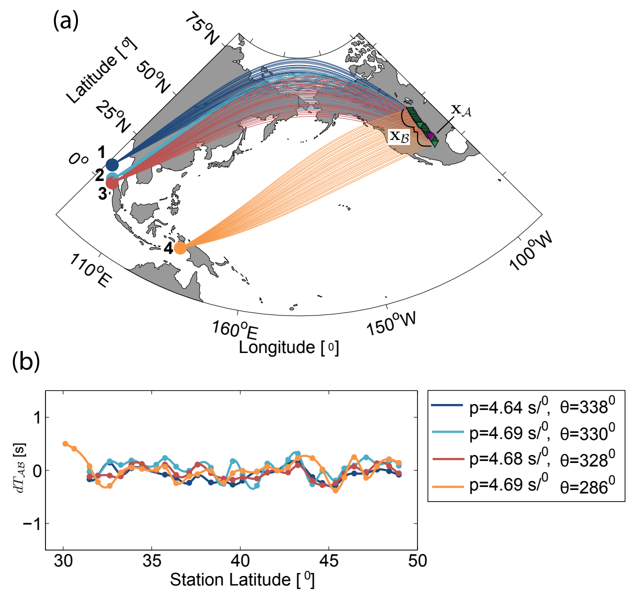

Figure A.1: Procedure for estimating an average rayparameter p for P_{diff}-raypaths over the Northern Pacific. (a) Depicts the configuration. The difficulty in reliably estimating p is that the apparent velocity of P_{diff} along the receiver array is affected by long-wavelength velocity variations near the array. Therefore, we use a linear array (green triangles) through the Great Plains, where little trend is expected in the receiver-side structure. For a collection of high-magnitude events from the Indonesian Archipelago (colored circles) we estimate –per event– a best-fitting line through the picked differential traveltimes (equation 4) and remove this linear trend, resulting in the functions as displayed in (b). The slope of the linear trends are an estimate of the rayparameter. The estimated rayparameters and the average backazimuths θ are shown on the right-hand side of (b). The mean and standard deviation of p are 4.66 and 0.028 s/deg, respectively.

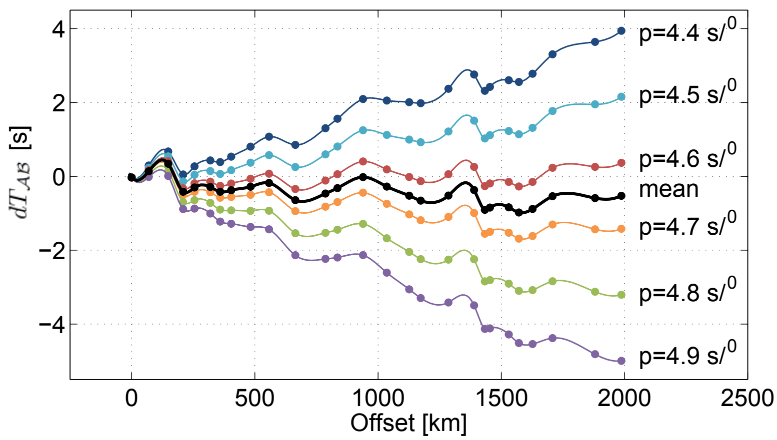

Figure A.2: The sensitivity of the extracted receiver-side anomaly $dT_{\mathcal{AB}}(\theta)$ to different linear-correction slopes p. The same source-and-receiver configuration is used as in Figure 2. The extracted receiver-side anomaly is plotted as function of distance with respect to the reference station $\mathbf{x}_{\mathcal{A}}$ (offset).

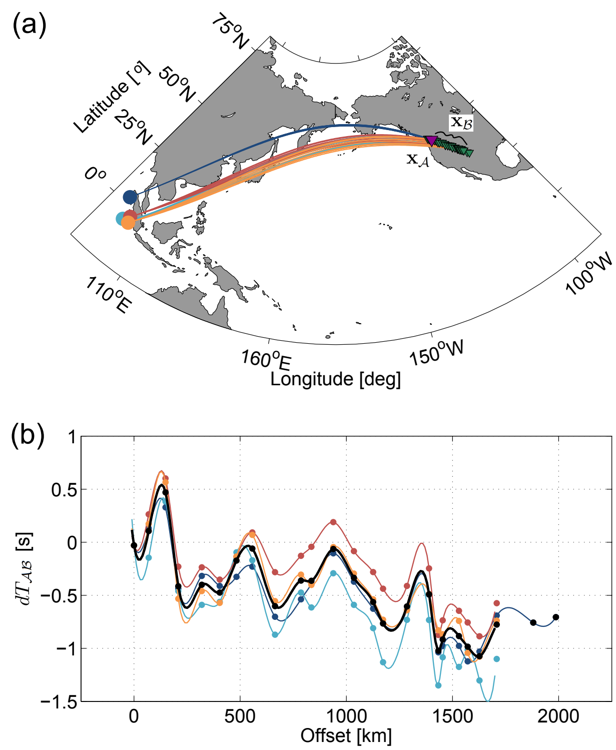

Figure A.3: Travel-time anomalies found with P_{diff} arrivals from four closely located earthquakes. (a) The configuration with the distribution of sources (circles) and receivers (green triangles) and the connecting great-circle paths (curved lines). The receiver array is the same as was used for Figure 2. Also, the earthquake denoted with the dark blue circle, is the same as was used for Figure 2. We show (b) the extracted travel-time anomalies as function of distance with respect to station $\mathbf{x}_{\mathcal{A}}$. The dots represent the extracted travel-time anomalies at the different stations, and the lines are created by spline interpolation of the dots. The black line is the average travel-time anomaly function. The standard deviation from the mean anomaly function is 0.163 s. The standard deviation from the mean linear trend is 0.010 s/deg.

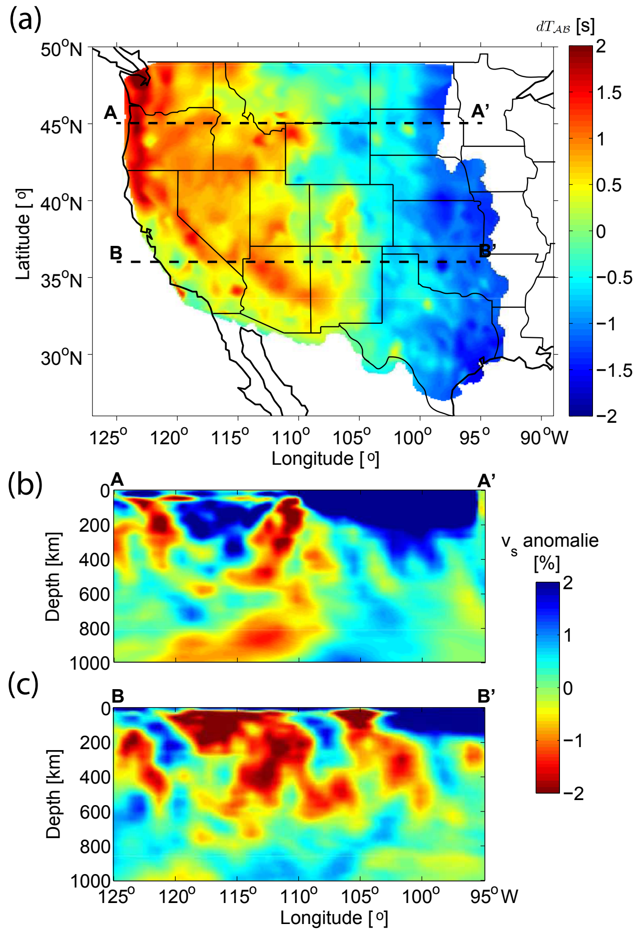

Figure A.4: Comparison of (a) the P_{diff} travel-time anomaly map with (b&c) two sections from DNAS-10S. The dashed lines in (a) denote the location of two cross-sections, A-A' (b) and B-B' (c). DNAS-10S is the most recent inversion model that incorporates the Great Plains [*Obrebski et al.*, 2011]. Although this is an S-wave model, *Schmandt and Humphreys* [2010] showed that similar features are resolved for a P-wave model. We extract two sections from DNAS-10S to compare with our anomaly map in depth. It is apparent that the features resolved in (a) come from an integration over depth of the features in (b) and (c). For example, the feeding channel for the Yellowstone volcanism (at about -113^0 longitude in (b)) extends far in depth, leading to a very slow anomaly in (a). The fast (blue) lithosphere block west of Yellowstone, however, does not lead to a fast anomaly in (a) since it is underlain by a slow anomaly in the lower mantle (at about 800 km in (b)). For a detailed interpretation of the anomalies in the Proterozoic part of the USA, we refer to *Obrebski et al.* [2011] and the references therein.

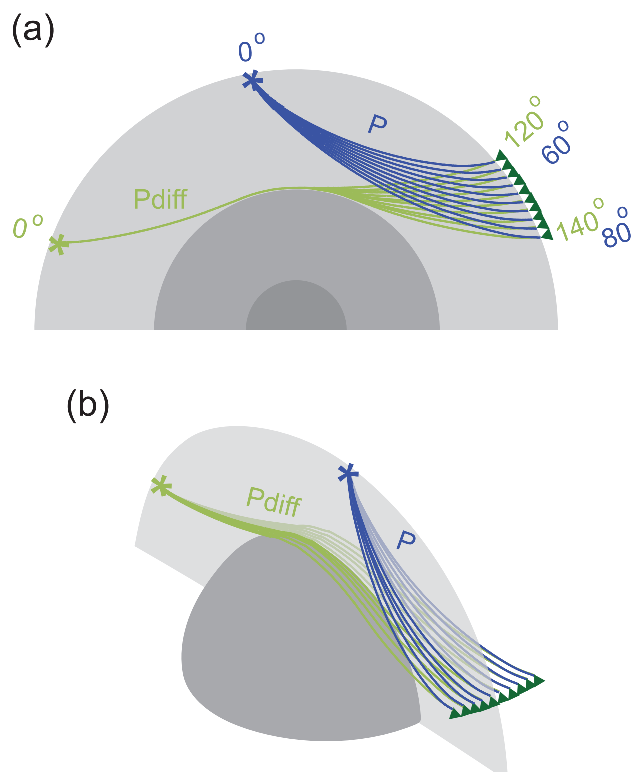

Figure A.5: Comparison of rayspreading for a P phase and a P_{diff} phase detected at a large array ($\Delta = 20^0$) of stations (green triangles). (a) and (b) show the rayspreading for an 'inline' and 'crossline' array, respectively.